Journal of the Operations Research
Society of Japan
2007, Vol. 50, No. 4, 540-562

QUADRATIC ORDERED MEDIAN LOCATION PROBLEMS

Yoshiaki Ohsawa
University of Tsukuba

Naoya Ozaki
Railway Technical Research Institute

Frank Plastria
Vrije Universiteit Brussel

Kazuki Tamura
Railway Technical Research Institute

(Received November 24, 2006; Revised August 22, 2007)

Abstract The criteria used in location analysis have to be chosen according to the character of the facility. The single facility location models addressed in this paper accommodate simultaneous multiple criteria in a continuous space in the framework of ordered median problems, which generate and unify many standard location problems. We demonstrate that tools of computational geometry such as Voronoi diagrams and arrangements of curves and lines, enable us to identify the entire set of Pareto-optimal locations, when the squared Euclidean distances between the facility and affected inhabitants are used. For two objectives this works for any type of ordered median objectives and any polygonally bounded feasible region. When more than two criteria are present the objectives and the feasible region have to be convex. For the analysis of this last case we extend several recent structural results for unconstrained convex vector optimization to a convex and compact constraint. Our findings are illustrated by several examples.

Keywords: Facility planning, location, multi-criteria, quadratic Euclidean distance, Pareto solutions, ordered median problem, Voronoi diagrams, arrangements of curves

1. Introduction

Recently, a great deal of effort in location theory has been spent on ordered median problems. This new type of location models is formulated in a quite general way to enhance their practical applicability. Many famous location problems can be regarded as special cases of this general model. Examples for attractive (or pull) facilities are Weber problems, center problems and cent-dian problems. Examples for obnoxious (or push) facilities are anticenter problems and anti-Weber problems. Examples for equity facilities are minimization of range and mean-difference. A comprehensive and detailed overview of ordered median problems can be found in the recent book by Nickel and Puerto[18]. In continuous space different distance measures have been incorporated in this framework, for example, rectilinear distance, and more generally polyhedral distance, by Kalcsics et al.[15], Nickel and Puerto[18], Puerto and Fernández[31], Rodríguez-Chía et al.[32], Rodríguez-Chía and Puerto[33], and Euclidean distance in Muñoz-Pérez and Saameño-Rodríguez[16].

On the other hand, there is a growing literature on multi-criteria approaches to optimize more than one objective function in location analysis with remarkable corresponding progress in mathematical programming, as can be seen in the survey by Nickel et al.[19].

This paper provides a unified structure for multi-criteria location models generated by combining continuous ordered median criteria with squared Euclidean distances. In fact, the two-objective models examined by Ohsawa[21], Ohsawa[22], Ohsawa et al.[23], Ohsawa et al.[24], Ohsawa and Tamura[25] can be regarded as special cases of this formulation. Their results are generalized and unified in the present framework using the subdivision of the feasible region into subregions where the objective function is either linear or quadratic.

We consider explicitly a bounded feasible region, which is not only necessary to apply the models to practical problems but also to ensure that optimal locations for push objectives exist. We present the computational complexity in terms of the total input size, i.e. the number of fixed points and the number of edges of the feasible region.

The research in this paper uses squared Euclidean distances, as in Ehrgott et al.[7], Fernández et al.[9], Francis and White[10], Ohsawa[21], Ohsawa et al.[23]. The main reason for this choice is of technical nature, because it allows to obtain analytical solutions for many problems; for the often more realistic Euclidean distance only few analytical results are available, even for the simple Weber problem. For some particular types of objectives both are equivalent, as will be seen later on, so our results then also hold for Euclidean distance; but this is rather exceptional. The second reason is that quadratic formulations generate simple circular level curves. This enables us to obtain an easy geographical view, somewhat similar to that obtained by a formulation using rectilinear distance which yields piecewise linear level curves, but without the disadvantage of axis dependency inherent in this latter. We therefore think that our formulation is quite useful to understand the essence of ordered median problems. It is hoped that these insights may help to study perhaps more realistic distance based models.

We start by characterizing the solution for *single-objective* squared Euclidean ordered median problems based on a Voronoi diagram. Muñoz-Pérez and Saameño-Rodríguez[16] examined undesirable Euclidean ordered median problems, that is, the weights which are assigned to affected inhabitants according to the ordered distances are all negative. Our solution method relaxes this assumption in the sense that some weights can be positive and the others can be negative.

Next, we present a procedure to identify the Pareto set and its related trade-off curves for the *two-objective* problem generated by combining two types of ordered median criteria, which may be both neither convex nor concave. As pointed out by many authors, e.g. Das and Dennis[4], it is only under convexity assumptions that minimization of various convex combinations of the original criteria succeeds in obtaining the whole set of Pareto-optimal locations. In fact, Hamacher and Nickel[12] and Nickel and Puerto[18] devote their discussion to convex two-objective location problems, so they consider only restricted situations. We are able to overcome this difficulty through tools of computational geometry such as Voronoi diagrams, combined with arrangements of curves and lines. We propose a solution method to solve *any* quadratic distance two-objective ordered median problem, even though each criterion and the feasible region might be non-convex.

Finally, we also develop an algorithm to produce all the two-dimensional Pareto-optimal locations associated with more than two convex ordered median criteria. To our knowledge, location models analytically dealing with more than two criteria are found only in Ehrgott et al.[7], Puerto and Fernández[29][30], Rodríguez-Chía and Puerto[33]. The first three works discuss particular problems, while in the last work a generic algorithm is described, but no concrete code nor its computational complexity are given. In contrast we fully describe an algorithm to generate the Pareto set for *any* multicriteria quadratic distance convex ordered median problem together with its computational complexity.

The paper is organized as follows. We begin with a study of single-objective ordered median problems in Section 2. Section 3 is devoted to the two-objective models generated by combining two ordered median problems. Section 4 describes the multi-objective models, which are defined on a convex polygonal region by combining more than two convex ordered median criteria. Finally, Section 5 gives a number of concluding remarks.

2. Single-Objective Models

2.1. Problem formulation

Consider a bounded region Ω on a Euclidean plane where a facility can be built. We assume its boundary $\partial\Omega$ consists of a finite number $|\partial\Omega|$ of straight-line segments. Let I and $\{\mathbf{p}_1, \mathbf{p}_2, \ldots, \mathbf{p}_{|I|}\}$ be the index and location sets of the affected inhabitants on the plane, respectively. We will use a boldfaced letter to represent sites. Let $\|\cdot\|$ be the Euclidean norm. Weights $\alpha_1, \alpha_2, \cdots, \alpha_i, \cdots, \alpha_{|I|}$ are assigned to the i-th nearest inhabitant from the facility. They can be negative values.

We deal with the following *quadratic distance ordered median problem* to place a facility somewhere in the feasible region Ω:

$$\min_{\mathbf{x}\in\Omega} \left(F(\mathbf{x}) \equiv \sum_{i\in I} \alpha_i \|\mathbf{x} - \mathbf{p}_{(i)}\|^2 \right), \tag{1}$$

where (i) is the index of the i-th nearest point from $\mathbf{x}$ among $\{\mathbf{p}_1, \ldots, \mathbf{p}_{|I|}\}$, implying that the indices (i) depend on the location $\mathbf{x}$; the explicit dependence of the (i)'s on $\mathbf{x}$ is suppressed for notational simplicity. In location terminology, problem (1) seeks to minimize the sum of weighted quadratic Euclidean distances between the facility and inhabitants, depending on the order of the distances from $\mathbf{x}$. Table 1 is based on the summary table of Nickel and Puerto[17] and the examples presented in Muñoz-Pérez and Saameño-Rodríguez[16] and includes several new proposals. The last column of this table is, however, fully valid only for squared Euclidean distances, see section 2.2 below. As suggested by the models in Table 1, the ordered median location problem generalizes and unifies many standard and less standard location problems. Clearly, when $\alpha_1 = \alpha_2 = \cdots = \alpha_{|I|} = 1$ the ordered median problem (1) reduces to the well-known Weber criterion. When $\alpha_1 = \alpha_2 = \cdots = \alpha_{|I|} = -1$ problem (1) becomes the anti-Weber criterion. In general the problems with $\alpha_i > 0$ for all $i \in I$ have pull objectives and can be applied to desirable facilities, and those with $\alpha_i < 0$ for all $i \in I$ have push objectives applicable to undesirable facilities. On the other hand, for $\alpha_1 = -\alpha_{|I|} > 0$ and $\alpha_2 = \cdots = \alpha_{|I|-1} = 0$ problem (1) corresponds to equity maximization using the range, as done by Drezner et al. [5]. Therefore, we see that the problem (1) is also applicable to equity location problems.

Note that when the set $\{\alpha_1, \alpha_2, \cdots, \alpha_{|I|}\}$ has only one nonzero element the problem (1) is equivalent to optimizing the corresponding objective function using simple (nonquadratic) Euclidean distance. Such problems are indicated by an asterisk in the second column of Table 1. In particular, when $|I|$ is odd, minimization of the median Euclidean distance is of this type, as the partial center problem with $n^+ = (|I| - 1)/2$. Note that for even $|I|$ the median distance is not uniquely defined, but this difficulty is often removed by using the middle median value, obtained as a trimmed mean with $m = |I|/2 - 1$; note, however, that the corresponding models with simple and squared distances then differ.

2.2. Properties

Voronoi diagrams are well studied concepts of Computational Geometry: see Okabe et al.[27], Ohyama[26]. Let $V_{i_1,i_2,\cdots,i_{|I|}}$ be the fully ordered Voronoi polygon (or cell) associated with the sequence $\mathbf{p}_{i_1}, \mathbf{p}_{i_2}, \cdots, \mathbf{p}_{i_{|I|}}$. It is mathematically expressed as

$$V_{i_1,i_2,\cdots,i_{|I|}} \equiv \{\mathbf{x} \in \mathbb{R}^2 \mid \|\mathbf{x} - \mathbf{p}_{i_1}\| \le \|\mathbf{x} - \mathbf{p}_{i_2}\| \le \cdots \le \|\mathbf{x} - \mathbf{p}_{i_{|I|}}\|\}. \tag{2}$$

This region is also called *ordered region* in Nickel and Puerto[17], Puerto and Fernández[31], Rodríguez-Chía et al.[32]. The *fully ordered Voronoi diagram* is defined as the collection

Table 1: Quadratic single-objective ordered median problems

criterion	problem	weights$(\alpha_1, \alpha_2, \cdots, \alpha_{\lvert I\rvert})$	sign of A	convexity
pull	Weber	$(1, 1, \cdots, 1, 1)$	$+$	convex
	center*	$(0, 0, \cdots, 0, 1)$	$+$	convex
	k-centrum	$(0, \cdots, 0, \overbrace{1, \cdots, 1}^{k})$	$+$	convex
	cent-dian	$(\omega, \omega, \cdots, \omega, 1), \quad (0 \le \omega \le 1)$	$+$	convex
	partial center*	$(0, \cdots, 0, 1, \overbrace{0, \cdots, 0}^{n^+})$	$+$	—
	trimmed mean	$(\overbrace{0, \cdots, 0}^{m}, 1, \cdots, 1, \overbrace{0, \cdots, 0}^{m})$	$+$	—
push	anti-Weber	$(-1, -1, \cdots, -1, -1)$	$-$	concave
	anticenter*	$(-1, 0, \cdots, 0, 0)$	$-$	—
	anti-k-centrum	$(\overbrace{-1, \cdots, -1}^{k}, 0, \cdots, 0)$	$-$	—
	anticenter-maxian	$(-1, -\omega, \cdots, -\omega, -\omega), \quad (0 \le \omega \le 1)$	$-$	—
	partial anticenter*	$(\overbrace{0, \cdots, 0}^{n^-}, -1, 0, \cdots, 0)$	$-$	—
	anti-trimmed mean	$(\overbrace{0, \cdots, 0}^{m}, -1, \cdots, -1, \overbrace{0, \cdots, 0}^{m})$	$-$	—
equity	mean difference	$(1 - \lvert I\rvert, 3 - \lvert I\rvert, \cdots, \lvert I\rvert - 3, \lvert I\rvert - 1)$	0	convex
	range	$(-1, 0, \cdots, 0, 1)$	0	convex
	trimmed range	$(\overbrace{0, \cdots, 0}^{m}, -1, 0, \cdots, 0, 1, \overbrace{0, \cdots, 0}^{m})$	0	—

of all non-empty $V_{i_1,i_2,\cdots,i_{|I|}}$'s (see Ohsawa et al.[23]). The cell-boundaries of this diagram coincide with the line tessellation generated by all the perpendicular bisectors of pairs $\mathbf{p}_i, \mathbf{p}_j$, which is explicitly used in Muñoz-Pérez and Saameño-Rodríguez[16]. This diagram refines and contains all types of order Voronoi diagrams such as standard and farthest-point Voronoi diagrams. We denote by ∂V the collection of the boundaries of $V_{i_1,i_2,\cdots,i_{|I|}}$'s within Ω.

Using the Voronoi region (2), $F(\mathbf{x})$ in (1) can be rewritten as

$$F(\mathbf{x}) \equiv \sum_{k\in I} \alpha_k \|\mathbf{x} - \mathbf{p}_{i_k}\|^2, \qquad \mathbf{x} \in V_{i_1,i_2,\cdots,i_{|I|}}. \tag{3}$$

Within $V_{i_1,i_2,\cdots,i_{|I|}}$ the indices i_k are independent of $\mathbf{x}$, contrary to (1). Therefore, when restricted to $V_{i_1,i_2,\cdots,i_{|I|}}$, we have a squared Euclidean distance problem, as examined by Drezner and Wesolowsky[6].

Define A by $A \equiv \sum_{k\in I} \alpha_k$. When $A = 0$, we may rewrite (3) as

$$F(\mathbf{x}) = \langle\ \mathbf{x}\ ;\ \hat{\mathbf{p}}_{i_1,i_2,\cdots,i_{|I|}}\ \rangle + \sum_{k\in I} \alpha_k \|\mathbf{p}_{i_k}\|^2, \qquad \mathbf{x} \in V_{i_1,i_2,\cdots,i_{|I|}}, \tag{4}$$

where

$$\hat{\mathbf{p}}_{i_1,i_2,\cdots,i_{|I|}} \equiv -2 \sum_{k\in I} \alpha_k \mathbf{p}_{i_k}. \tag{5}$$

Thus, $F(\mathbf{x})$ is piecewise linear, with pieces $V_{i_1,i_2,\cdots,i_{|I|}}$ within which its contours are parallel lines orthogonal to $\hat{\mathbf{p}}_{i_1,i_2,\cdots,i_{|I|}}$.

When $A \neq 0$ the following equivalent formulation of (3) can be found in Francis and White [10]:

$$F(\mathbf{x}) = A\|\mathbf{x} - \overline{\mathbf{p}}_{i_1,i_2,\cdots,i_{|I|}}\|^2 + \sum_{k\in I} \alpha_k \|\mathbf{p}_{i_k} - \overline{\mathbf{p}}_{i_1,i_2,\cdots,i_{|I|}}\|^2, \qquad \mathbf{x} \in V_{i_1,i_2,\cdots,i_{|I|}}, \tag{6}$$

where

$$\bar{\mathbf{p}}_{i_1,i_2,\cdots,i_{|I|}} \equiv \frac{1}{A}\sum_{k\in I} \alpha_k \mathbf{p}_{i_k} = -\frac{1}{2A}\hat{\mathbf{p}}_{i_1,i_2,\cdots,i_{|I|}}. \tag{7}$$

It follows that minimizing $F(\mathbf{x})$ is equivalent to minimizing (when $A > 0$) or maximizing (when $A < 0$) $\|\mathbf{x} - \overline{\mathbf{p}}_{i_1,i_2,\cdots,i_{|I|}}\|^2$.

This yields three main observations about the objective function (3). First, unless $A = 0$, the level sets of $F(\mathbf{x})$ within the Voronoi polygon $V_{i_1,i_2,\cdots,i_{|I|}}$ are circular arcs centered at the center of gravity $\bar{\mathbf{p}}_{i_1,i_2,\cdots,i_{|I|}}$ and with a radius of

$$\sqrt{\frac{F(\mathbf{x}) - \sum_{k\in I}\alpha_k \left(\|\mathbf{p}_{i_k} - \overline{\mathbf{p}}_{i_1,i_2,\cdots,i_{|I|}}\|\right)^2}{|A|}}.$$

Second, when $A > 0$, $F(\mathbf{x})$ is strictly convex within each Voronoi polygon, while for $A < 0$, $F(\mathbf{x})$ is strictly concave within them. Thus, the sign of A plays an important role determining simply and geometrically the region-wise functional forms. In addition, for $A > 0$ ($A < 0$), $F(\mathbf{x})$ increases (decreases) with the distance $\|\mathbf{x} - \overline{\mathbf{p}}_{i_1,i_2,\cdots,i_{|I|}}\|$. Therefore, in the context of facility planning, $F(\mathbf{x})$ may be regarded as a pull objective in case $A > 0$, while for $A < 0$ it should rather be regarded as a push objective. When $A = 0$ $F(\mathbf{x})$ may be seen as an equity criterion. The mean difference and the range are examined in Ohsawa et al.[23], Drezner et al.[5], respectively.

Finally, the function $F(\mathbf{x})$ is in general non-convex and multiple optimal solutions may arise. As the contour plots in Ohsawa et al.[24] clearly show, partial center and partial anticenter problems can be non-convex. It is readily verified that the trimmed mean and range problems can be neither convex nor concave. However, based on Crouzeix and Kebbour[3], $F(\mathbf{x})$ is strictly convex as soon as $0 \leq \alpha_1 \leq \alpha_2 \leq \cdots \leq \alpha_{|I|}$. Consequently, many pull objectives are strictly convex. The objective functions of mean difference and range are both convex. This is because they can be rewritten as $\sum_{i\in I}\sum_{j\in I} |\|\mathbf{x} - \mathbf{p}_i\|^2 - \|\mathbf{x} - \mathbf{p}_j\|^2|$ and $\max_{i,j\in I} |\|\mathbf{x} - \mathbf{p}_i\|^2 - \|\mathbf{x} - \mathbf{p}_j\|^2|$, respectively, and $|\|\mathbf{x} - \mathbf{p}_i\|^2 - \|\mathbf{x} - \mathbf{p}_j\|^2|$ is convex.

Define $\bar{P}$ as the set obtained by taking, for each permutation of the index set, the (unique) point of $V_{i_1,i_2,\cdots,i_{|I|}} \cap \Omega$ closest to $\bar{\mathbf{p}}_{i_1,i_2,\cdots,i_{|I|}}$, i.e., $\bar{\mathbf{p}}_{i_1,i_2,\cdots,i_{|I|}}$ itself or its nearest projection point on $V_{i_1,i_2,\cdots,i_{|I|}} \cap \Omega$.

Proposition 1 *When $A > 0$ any minimum point $\mathbf{f}^*$ of $F(\mathbf{x})$ lies in $\bar{P}$. Otherwise, such a $\mathbf{f}^*$ may be found at some vertex of $\partial V \cup \partial\Omega$.*

Proof If $A > 0$, the objective $F(\mathbf{x})$ is strictly convex on each $V_{i_1,i_2,\cdots,i_{|I|}}$, so the constrained minimum $\mathbf{f}^*$ of $F(\mathbf{x})$ on $V_{i_1,i_2,\cdots,i_{|I|}} \cap \Omega$ is unique, and by (6) lies in $\bar{P}$. Therefore any global solution $\mathbf{f}^*$ is an element of the set $\bar{P}$.
In case $A \leq 0$, $F(\mathbf{x})$ is concave. This means that the optimal value of $F(\mathbf{x})$ on $V_{i_1,i_2,\cdots,i_{|I|}}$ will be reached at some extreme point of (the convex hull of) $V_{i_1,i_2,\cdots,i_{|I|}} \cap \Omega$. Such an extreme point is always a vertex of $\partial V \cup \partial\Omega$. ∎

Observe that concave vertices of Ω which are not on ∂V will never be an extreme point of any $V_{i_1,i_2,\cdots,i_{|I|}} \cap \Omega$, so should not be considered.

In particular this proposition states that optimal solutions may always be found either at some $\bar{\mathbf{p}}_{i_1,i_2,\cdots,i_{|I|}}$ or in $\partial V \cup \partial\Omega$. This result generalizes the findings for partial center and partial anticenter problems formulated by Ohsawa et al.[24], and those for minimization of the mean-difference examined by Ohsawa et al.[23]. Our result is analogous to Theorem 4.5 of Nickel and Puerto[18] under rectilinear ordered median problems. When $\alpha_i < 0$ for all $i \in I$ it is consistent with the finding using a simple Euclidean distance by Muñoz-Pérez and Saameño-Rodríguez[16].

2.3. Solution procedure

It follows from Proposition 1 that we may restrict our search to a finite set of candidate points, leading to the following method to obtain an optimal location:

Algorithm 1

Step 1. Set up the planar graph $\partial V \cup \partial\Omega$.

Step 2. Find the minimum point of $F(\mathbf{x})$ among $\bar{P}$ when $A > 0$, or among the nodes of the graph $\partial V \cup \partial\Omega$ in case $A \leq 0$.

Proposition 2 *A solution* $\mathbf{f}^*$ *can be found in* $O(|I|^5 + |I|^3|\partial\Omega|)$ *time.*

Proof A square which contains Ω can be defined in $O(|\partial\Omega|)$. We can construct the Voronoi diagram within the square in $O(|I|^4)$, as shown in Algorithm 1 of Ohsawa et al.[23]. We can cut off $\partial V \cup \partial\Omega$ from this Voronoi diagram in $O(|I|^2|\partial\Omega|)$ time. Thus, the graph $\partial V \cup \partial\Omega$ can be defined in $O(|I|^4 + |I|^2|\partial\Omega|)$ time, so Step 1 takes $O(|I|^4 + |I|^2|\partial\Omega|)$. The graph has $O(|I|^4 + |I|^2|\partial\Omega|)$ faces, and each center of gravity $\bar{\mathbf{p}}_{i_1,i_2,\cdots,i_{|I|}}$ can be identified in $O(|I|)$ based on (7), in total this takes $O(|I|^5+|I|^3|\partial\Omega|)$ time. Determining all the projection points of these centers of gravity on their corresponding cell involves inspection of each the $O(|I|^4 + |I|^2|\partial\Omega|)$ edges of the planar graph $\partial V \cup \partial\Omega$ at most twice, so this part of the task is dominated by the previous one. There are $O(|I|^4 + |I|^2|\partial\Omega|)$ candidate points for the optimal solution. Using (3), each candidate can be evaluated in $O(|I|)$. Therefore, Step 2 can be done in $O(|I|^5 + |I|^3|\partial\Omega|)$, which equals the total time complexity. ∎

Note that if the feasible region Ω is convex, the complexity can be reduced to $O(|I|^5 + |I||\partial\Omega|)$ time, as shown in Proposition 4 in Ohsawa et al.[23].

2.4. Computational experiments

We will illustrate the intuition behind our models by use of a real-world example. Suppose that Ibaraki Prefecture in Japan would construct one desirable and one undesirable facility within it to serve its inhabitants. The desirable facility is built based on the following k-centrum problem, which minimizes the sum of the squared Euclidean distances between the facility and the k farthest inhabitants: see Slater[34]. Its formulation is

$$\min_{\mathbf{x}\in\Omega} \left(\max_{\overline{I}\subseteq I, |\overline{I}|=k} \sum_{i\in\overline{I}} \|\mathbf{x} - \mathbf{p}_i\|^2 \right).$$

A generalization of this objective is examined in Ogryczak and Tamir[20], Tamir[35].

The undesirable facility is constructed according to the anti-k-centrum problem, which is formulated in Muñoz-Pérez and Saameño-Rodríguez[16]. This problem is to maximize

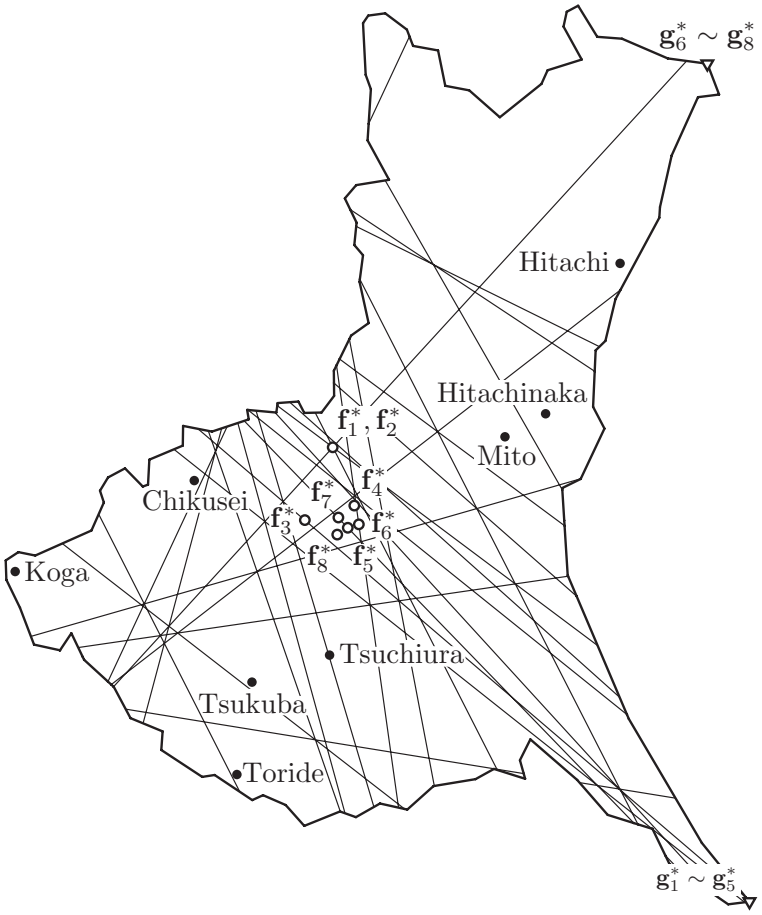

Figure 1: Graph $\partial V \cup \partial\Omega$ and solutions $\mathbf{f}_k^*$, $\mathbf{g}_k^*$ $(k = 1, \ldots, 8)$

the sum of the distances between the facility and the k closest inhabitants as follows:

$$\max_{\mathbf{x}\in\Omega} \left(\min_{\overline{I}\subseteq I, |\overline{I}|=k} \sum_{i\in\overline{I}} \|\mathbf{x} - \mathbf{p}_i\|^2 \right).$$

As indicated in Table 1, both problems belong to the quadratic ordered median problems. As special cases, if $k = |I|$, then the former problem reduces to the quadratic distance variant of the well-known Weber problem, and the latter one reduces to the anti-Weber problem. If $k = 1$, the former problem reduces to the center problem, and the latter one reduces to the anti-center problem. We analyze how changing k affects optimal locations.

The location data of our example are shown in Figure 1. The affected points are eight municipalities with a population of more than 100,000 people in the Ibaraki prefecture on April 1, 2006. They are indicated as bullets in Figure 1. The lines indicate the fully ordered Voronoi diagram within the prefecture. The optimal solutions $\mathbf{f}_k^*$ for each k-centrum problem $(k = 1, \ldots, 8)$ are shown as circles. The solution $\mathbf{f}_1^*$ coincides with the center, which is the circumcenter of Hitachi, Koga and Toride. The solution $\mathbf{f}_8^*$ is the center of gravity of the eight municipalities, since it lies within Ω. We recognize from this figure that the solutions are all located in the central area of the prefecture, even though an increase in k changes slightly the solutions. Note that the solutions $\mathbf{f}_4^*$ and $\mathbf{f}_8^*$ are inner cell-points of V, and the others are on the boundary ∂V. Only $\mathbf{f}_1^* = \mathbf{f}_2^*$ are on a vertex of the boundary ∂V.

The solutions $\mathbf{g}_k^*$ for the anti-k-centrum problem are denoted as triangles in Figure 1. We see from this figure that the eight optimal solutions are restricted to only two places, and that the solution moves suddenly from the southeast corner of the prefecture to its northeast corner as the parameter k is increased from 5 to 6.

3. Two-Objective Models

3.1. Problem formulation

In addition to the ordered median problem (1), we consider a second ordered median problem with weights $\beta_1, \beta_2, \cdots, \beta_{|I|}$:

$$\min_{\mathbf{x}\in\Omega} \left(G(\mathbf{x}) \equiv \sum_{i\in I} \beta_i \|\mathbf{x} - \mathbf{p}_{(i)}\|^2 \right). \tag{8}$$

In analogy to $\mathbf{f}^*$, A, $\hat{\mathbf{p}}_{i_1,i_2,\cdots,i_{|I|}}$ and $\bar{\mathbf{p}}_{i_1,i_2,\cdots,i_{|I|}}$, we define the notations $\mathbf{g}^*$, B, $\hat{\mathbf{q}}_{i_1,i_2,\cdots,i_{|I|}}$ and $\bar{\mathbf{q}}_{i_1,i_2,\cdots,i_{|I|}}$ for $G(\mathbf{x})$ similarly.

We consider the following *quadratic two-objective ordered median problem*, which is obtained by combining the two ordered median objectives (1) and (8):

$$\min_{\mathbf{x}\in\Omega} \{F(\mathbf{x}), G(\mathbf{x})\}. \tag{9}$$

Pareto-optimal locations are such that no other feasible location exists which is at least as good for one criterion and strictly better for the other criterion. We call the set of all Pareto-optimal locations the *Pareto set* and denote it by E^*. Using the notation $(F,G)(S) \equiv \{(F(\mathbf{x}), G(\mathbf{x}))|\mathbf{x} \in S\}$ for any set $S \subseteq \Omega$, we obtain the image in the objective space $(F,G)(\Omega)$ and its lower-left envelope, which is the *trade-off curve* $(F,G)(E^*)$ (except for some exceptionally possible vertical or horizontal pieces). As in much of the multi-criteria literature, we consider that solving the location problem means deriving the full Pareto set and its corresponding trade-off curve. Typically E^* will be a (possibly discontinuous and/or multiple) trajectory with extremes $\mathbf{f}^*$, $\mathbf{g}^*$.

Table 2: Quadratic two-objective ordered median problems

criteria	single-objective problems	convexity	reference
pull vs. pull	Weber vs. center	convex	[21]
pull vs. push	center vs. anti-center		[22]
	partial anti-center vs. partial center		[24]
pull vs. equity	Weber vs. mean difference	convex	[23]
push vs. equity	anti-Weber vs. mean difference	concave	[23]

As shown in Table 2, some special cases of our formulation (9) have already been investigated. An interesting special case of this formulation is the cent-dian problem: see Ohsawa[21]. Other interesting special cases are the partial anti-center and partial center problems, where both criteria are neither convex nor concave: see Ohsawa et al.[24].

In order to restrict the number of possibilities that need to be considered, some non-generic particular cases are eliminated by assuming that the points $\mathbf{p}_{i_1,i_2,\cdots,i_{|I|}}$ are in general position in the sense that

(a-1) any contour line of $F(\mathbf{x})$ intersects any contour line of $G(\mathbf{x})$ in isolated points only;

(a-2) both $F(\mathbf{x})$ and $G(\mathbf{x})$ have unique minimum solutions.

It goes without saying that not all of these assumptions are needed for all results. In real applications using actual location data, our assumptions will almost always hold. Therefore, we can make these assumptions without loss of real-world applicability.

3.2. Properties

For each $V_{i_1,i_2,\cdots,i_{|I|}}$, we define the line $L_{i_1,i_2,\cdots,i_{|I|}}$ as follows:

$$L_{i_1,i_2,\cdots,i_{|I|}} = \begin{cases} \text{the line through } \bar{\mathbf{p}}_{i_1,i_2,\cdots,i_{|I|}} \text{ and } \bar{\mathbf{q}}_{i_1,i_2,\cdots,i_{|I|}}, & \text{if } AB \neq 0, \\ \text{the line through } \bar{\mathbf{q}}_{i_1,i_2,\cdots,i_{|I|}} \text{ in the direction } \hat{\mathbf{p}}_{i_1,i_2,\cdots,i_{|I|}}, & \text{if } A = 0 \text{ and } B \neq 0, \\ \text{the line through } \bar{\mathbf{p}}_{i_1,i_2,\cdots,i_{|I|}} \text{ in the direction } \hat{\mathbf{q}}_{i_1,i_2,\cdots,i_{|I|}}, & \text{if } A \neq 0 \text{ and } B = 0. \end{cases}$$

Define the set L as the union of all sets $L_{i_1,i_2,\cdots,i_{|I|}} \cap V_{i_1,i_2,\cdots,i_{|I|}} \cap \Omega$ for all permutations of the index set with $V_{i_1,i_2,\cdots,i_{|I|}} \neq \emptyset$.

Proposition 3 *The Pareto set E^* is a subset of $\partial V \cup L \cup \partial\Omega$.*

Proof Unless a Pareto-optimal location is situated at the boundary of the Voronoi region $\partial V \cup \partial\Omega$, it must be a position where the contour of $F(\mathbf{x})$ and that of $G(\mathbf{x})$ are tangent. The former contour is either part of the circle with center at $\bar{\mathbf{p}}_{i_1,i_2,\cdots,i_{|I|}}$ in case $A \neq 0$ or otherwise a line-segment orthogonal to $\hat{\mathbf{p}}_{i_1,i_2,\cdots,i_{|I|}}$. Similarly the latter is either a circular arc with center at $\bar{\mathbf{q}}_{i_1,i_2,\cdots,i_{|I|}}$ in case $B \neq 0$ or otherwise a line-segment orthogonal to $\hat{\mathbf{q}}_{i_1,i_2,\cdots,i_{|I|}}$. Because of assumption (a-1), such a tangent position, i.e., the touching point of two contours, has to lie on a line segment $L_{i_1,i_2,\cdots,i_{|I|}}$. ∎

One may also observe more precisely that in case $AB > 0$, the candidates can be limited to the line segments connecting $\bar{\mathbf{p}}_{i_1,i_2,\cdots,i_{|I|}}$ and $\bar{\mathbf{q}}_{i_1,i_2,\cdots,i_{|I|}}$. When $AB < 0$ one may restrict search to the parts of the connecting lines outside these line segments. However, this more detailed information does not seem to be useful to reduce computational complexity. Proposition 3 states that we may restrict our search to the edges of the planar graph $\partial V \cup L \cup \partial\Omega$, indicating the noteworthy property that the Pareto set E^* has to be a polygonal path.

3.3. Solution procedure

Clearly, $\partial V \cup \partial\Omega \cup L$ may contain locations that cannot be Pareto-optimal. Accordingly, the Pareto set has still to be constructed within $\partial V \cup \partial\Omega \cup L$. The trade-off curve is given by the lower-left envelope of $(F, G)(\partial V \cup \partial\Omega \cup L)$. Hence, the Pareto set E^* and its corresponding trade-off curve can be constructed by the following algorithm, which generalizes and unifies the methods by Ohsawa[21][22], Ohsawa et al.[23], Ohsawa et al.[24].

Algorithm 2

Step 1. Construct the planar graph $\partial V \cup L \cup \partial\Omega$.

Step 2. Delineate the loci of $(F, G)(\partial V \cup L \cup \partial\Omega)$ for the graph in objective space.

Step 3. Detect the lower-left envelope of the loci.

Step 4. Specify the parts which lie in the envelope in the geographical space.

Proposition 4 *The Pareto set E^* and the trade-off curve $(F, G)(E^*)$ can be found in $O((|I|^4 + |I|^2|\partial\Omega|)(|I| + \log|\partial\Omega|))$ time.*

Proof We can find a square which contains Ω in $O(|\partial\Omega|)$ time. By applying Step 1 of Algorithm 2 in Ohsawa et al.[23], the graph consisting of Voronoi edges and lines containing all line segments of L within the square can be defined in $O(|I|^5 + |I||\partial\Omega|)$. We can cut

off $\partial V \cup L \cup \Omega$ from the graph by traversing along $\partial\Omega$ in $O(|I|^2|\partial\Omega|)$. Thus, Step 1 has complexity $O(|I|^5 + |I|^2|\partial\Omega|)$. Since the graph $\partial V \cup L \cup \partial\Omega$ has $O(|I|^4 + |I|^2|\partial\Omega|)$ edges, while using (3), Step 2 can be accomplished in $O(|I|^5 + |I|^3|\partial\Omega|)$ time, which dominates the complexity of Step 1.

To define the envelope of the loci $(F, G)(\partial V \cup L \cup \partial\Omega)$, it is necessary to repeatedly identify where a pair of loci intersect. We consider the case of $AB \neq 0$. Let $\mathbf{p}'$ and $\mathbf{q}'$ be the projections of $\bar{\mathbf{p}}_{i_1,i_2,\cdots,i_{|I|}}$ and $\bar{\mathbf{q}}_{i_1,i_2,\cdots,i_{|I|}}$ onto a line l on $V_{i_1,i_2,\cdots,i_{|I|}}$, respectively. It follows from these definitions and equation (6) that any location $\mathbf{x}$ on $l \cap V_{i_1,i_2,\cdots,i_{|I|}}$ takes

$$F(\mathbf{x}) = A\|\mathbf{x} - \mathbf{p}'\|^2 + C_1, \tag{10}$$
$$G(\mathbf{x}) = B\|\mathbf{x} - \mathbf{q}'\|^2 + C_2, \tag{11}$$

where

$$C_1 \equiv A\|\mathbf{p}' - \bar{\mathbf{p}}_{i_1,i_2,\cdots,i_{|I|}}\|^2 + \sum_{k\in I} \alpha_k \|\mathbf{p}_{i_k} - \overline{\mathbf{p}}_{i_1,i_2,\cdots,i_{|I|}}\|^2,$$
$$C_2 \equiv B\|\mathbf{q}' - \bar{\mathbf{q}}_{i_1,i_2,\cdots,i_{|I|}}\|^2 + \sum_{k\in I} \beta_k \|\mathbf{p}_{i_k} - \overline{\mathbf{q}}_{i_1,i_2,\cdots,i_{|I|}}\|^2.$$

If $\mathbf{p}' = \mathbf{q}'$, following from (10) and (11), we have

$$G(\mathbf{x}) = \frac{B}{A}(F(\mathbf{x}) - C_1) + C_2,$$

indicating that $G(\mathbf{x})$ can be expressed as a term linear in $F(\mathbf{x})$. Otherwise, parametrising the line l by $\mathbf{x} = (1-t)\mathbf{p}' + t\mathbf{q}'$, substituting this into (10) and (11) yields

$$F(\mathbf{x}) = A\|\mathbf{p}' - \mathbf{q}'\|^2 t^2 + C_1,$$
$$G(\mathbf{x}) = B\|\mathbf{p}' - \mathbf{q}'\|^2 (1-t)^2 + C_2.$$

Eliminating t from the two equations (10) and (11), we have

$$G(\mathbf{x}) = \frac{B}{A}(F(\mathbf{x}) - C_1) + C_3\sqrt{F(\mathbf{x}) - C_1} + C_4,$$

where

$$C_3 \equiv \pm\frac{2B\|\mathbf{p}' - \mathbf{q}'\|}{\sqrt{A}},$$
$$C_4 \equiv C_2 - B\|\mathbf{p}' - \mathbf{q}'\|^2.$$

Note that the constants A and B are independent of $V_{i_1,i_2,\cdots,i_{|I|}}$. Therefore, when eliminating $G(\mathbf{x})$ from two different of such equations, one obtains either a linear or a quadratic equation in $F(\mathbf{x})$, which has at most two solutions. This means that the two loci of edges of $(F, G)(\partial V \cup L \cup \partial\Omega)$ intersect each other at most twice. Thus, Step 3 requires $O((|I|^4 + |I|^2|\partial\Omega|)\log(|I|^4 + |I|^2|\partial\Omega|))$ time.

Since the graph $\partial V \cup L \cup \partial\Omega$ has $O(|I|^4 + |I|^2|\partial\Omega|)$ edges, the complexity of Step 4 is $O(|I|^4 + |I|^2|\partial\Omega|)$. Noting that $O(|I|^5 + |I|^3|\partial\Omega|) + O((|I|^4 + |I|^2|\partial\Omega|)\log(|I|^4 + |I|^2|\partial\Omega|)) = O((|I|^4 + |I|^2|\partial\Omega|)(|I| + \log|\partial\Omega|))$, the proof is complete. ∎

Three additional remarks may be made. First, when Ω is a convex region, the complexity can be reduced to $O((|I|^4 + |\partial\Omega|)(|I| + \log|\partial\Omega|))$ time, as discussed in Ohsawa et

al.[23]. Second, if $F(\mathbf{x})$ and $G(\mathbf{x})$ are both convex, an algorithm with lower computational complexity than Algorithm 2 may be designed along the lines described in Ohsawa et al.[23]. This variant will also shortly be described in Section 4. Finally, Algorithm 2 works irrespective of convexity of the two objective functions. Accordingly, the algorithm is applicable in particular to semi-obnoxious facility location, as examined by, for example, Carrizosa and Plastria[2].

3.4. Computational experiments

We consider two types of such semi-obnoxious facility location problems which both focus on the trade-off between undesirable and desirable effects. For convenience, we use the location data used in Ohsawa et al.[24], where there are only five affected points. The first problem is given as follows:

$$\min_{\mathbf{x}\in\Omega}\{F^1(\mathbf{x}), G^1(\mathbf{x})\}, \tag{12}$$

where,

$$F^1(\mathbf{x}) \equiv -\max_{\bar{I}\subseteq I,|\bar{I}|=|I|-2}\left(\min_{i\in\bar{I}}\|\mathbf{x}-\mathbf{p}_i\|^2\right), \tag{13}$$

$$G^1(\mathbf{x}) \equiv \sum_{i\in I}\|\mathbf{x}-\mathbf{p}_i\|^2 + \max_{i\in I}\|\mathbf{x}-\mathbf{p}_i\|^2. \tag{14}$$

Criterion (13) is a partial anti-center problem, in which two inhabitants are neglected when determining facility location. Thus, this criterion takes an undesirable point of view, seeking to maximize the nearest distance from the facility to $|I|-2$ inhabitants. On the other hand, the latter criterion (14) is a cent-dian problem with the parameter $\omega = 0.5$ in Table 1. This is a classical problem for locating a desirable facility, whose idea is proposed by Halpern[11], and axiomatically studied by Carrizosa et al.[1].

The second problem we take up is:

$$\min_{\mathbf{x}\in\Omega}\{F^2(\mathbf{x}), G^2(\mathbf{x})\}, \tag{15}$$

where,

$$F^2(\mathbf{x}) \equiv -\left(\sum_{i\in I}\|\mathbf{x}-\mathbf{p}_i\|^2 + \min_{i\in I}\|\mathbf{x}-\mathbf{p}_i\|^2\right), \tag{16}$$

$$G^2(\mathbf{x}) \equiv \min_{\bar{I}\subseteq I,|\bar{I}|=|I|-2}\left(\max_{i\in\bar{I}}\|\mathbf{x}-\mathbf{p}_i\|^2\right). \tag{17}$$

The former criterion (16) is an anti-center-maxian problem with the parameter $\omega = 0.5$ in Table 1, which is proposed in Eiselt and Laporte[8]. This is applicable for the determination of the location of an undesirable facility. On the other hand, the latter criterion (17) is a partial center problem, where two inhabitants are not considered in the decision making. Thus, the criterion takes a desirable point of view and seeks to minimize the farthest distance from the facility to $|I|-2$ inhabitants.

Thus, in both problems (12) and (15), the facility location is determined based on a trade-off between pull and push forces. Two observations may be made. First, $F^1(\mathbf{x})$ and $G^2(\mathbf{x})$ are both non-concave and non-convex, although $G^1(\mathbf{x})$ is convex and $F^2(\mathbf{x})$ is concave. Second, the Pareto set associated with $F^1(\mathbf{x})$ and $G^2(\mathbf{x})$ is examined in Ohsawa et al.[24], where only two types of Voronoi diagrams are used, but here the line tessellation is

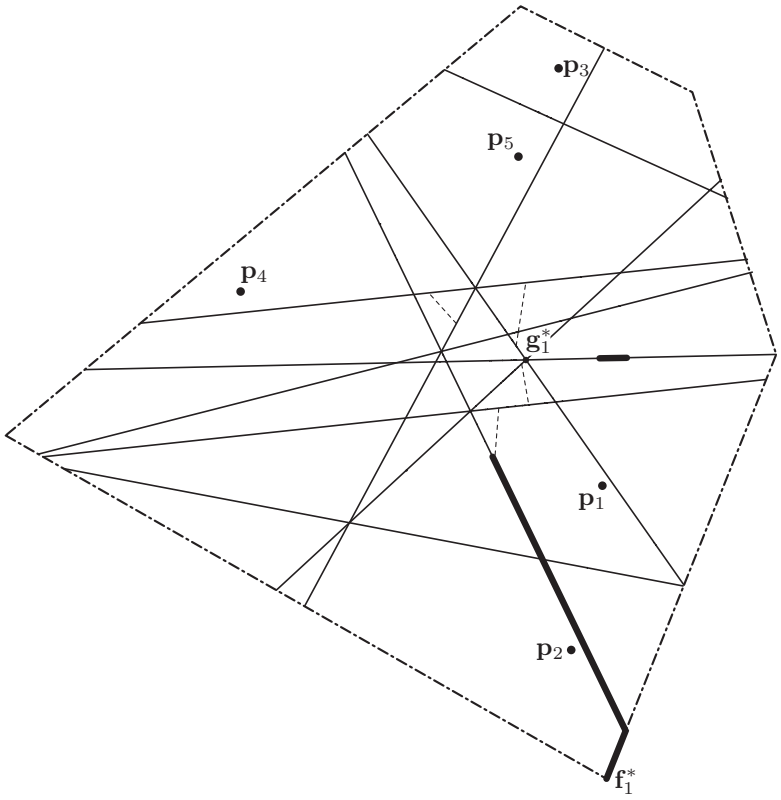

Figure 2: Pareto set for partial anticenter with cent-dian criteria

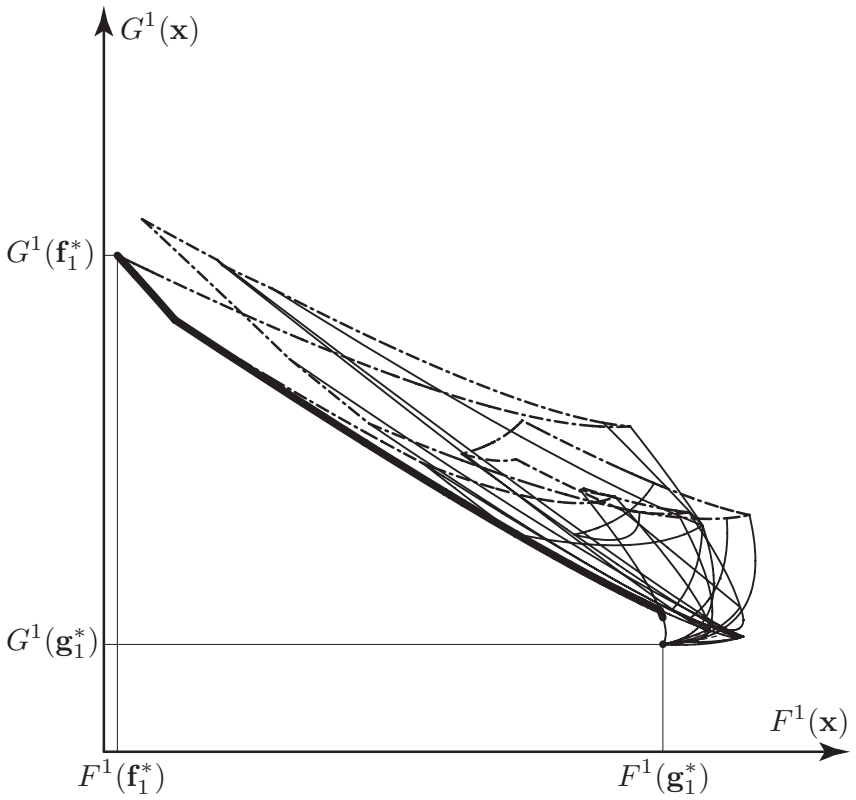

Figure 3: Trade-off curve for partial anticenter with cent-dian criteria

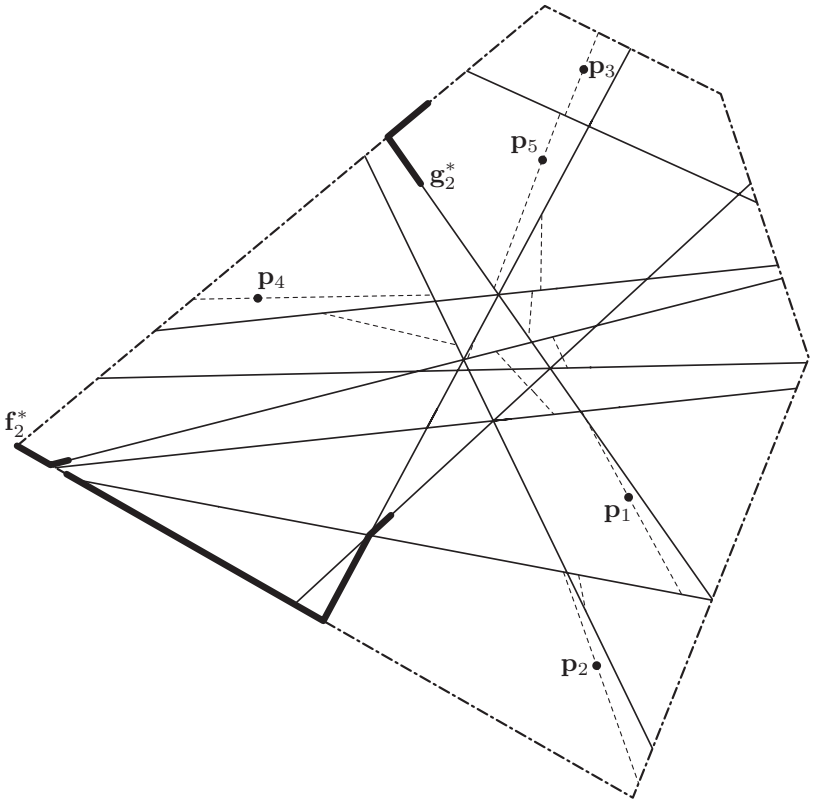

Figure 4: Pareto set for anticenter-maxion with partial covering criteria

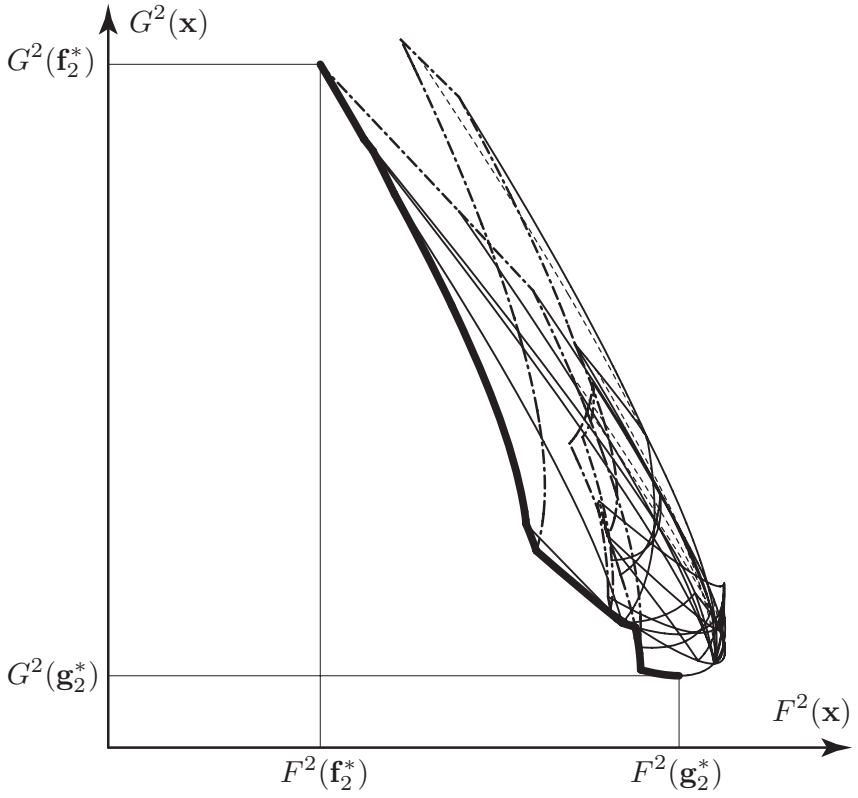

Figure 5: Trade-off curve for anticenter-maxion with partial covering criteria

necessary to solve the problem in order to use our solution method. This is because Weber and anti-Weber criteria are calculated on all the inhabitant location data.

There are five affected points, indicated by the $\mathbf{p}_i$. The graph $\partial V \cup L \cup \partial\Omega$ for the first two-objective problem (12) is shown in Figure 2, where the sets ∂V, L and $\partial\Omega$ are indicated by thin, broken and chain lines, respectively. Note that in the partial anti-center problem, $\bar{\mathbf{p}}_{i_1,i_2,\cdots,i_{|I|}}$ which defines $L_{i_1,i_2,\cdots,i_{|I|}}$ coincides with a point of $\mathbf{p}_i$'s, because there is only one non-zero α_i. Hence, every straight line containing broken lines shown in Figure 2 passes through a point of $\mathbf{p}_i$'s. The loci of $(F,G)(\partial V \cup L \cup \partial\Omega)$ are plotted in Figure 3 with the horizontal and vertical axes measuring values of F and G, respectively. As in Figure 2, the loci $(F,G)(\partial V)$, $(F,G)(L)$ and $(F,G)(\partial\Omega)$ are shown by thin, broken and chain lines, respectively. The lower envelope of the loci is indicated as solid curves. The corresponding Pareto set E^* is described by solid segments in Figure 2. The set E^* consists of one isolated point, which is the minimizer of $G^1(\mathbf{x})$, i.e., $\mathbf{g}_1^*$, and two disconnected curve-segments. The optimal solution of $F^1(\mathbf{x})$, i.e., $\mathbf{f}_1^*$ is located at the endpoint of the bent segment. As is evident on referring to Figure 3, the trade-off curve $(F,G)(E^*)$, that is, the conflicts between the criteria F and G, is discontinuous. One part contains $(F,G)(\mathbf{f}_1^*)$, and another contains $(F,G)(\mathbf{g}_1^*)$.

Similarly, the graph $\partial V \cup L \cup \partial\Omega$ and the Pareto set E^* for the second two-objective problem (15) are shown in Figure 4. Note that ∂V in Figure 2 coincides with ∂V in Figure 4. The third nearest-point Voronoi diagram is the same as the third farthest-point Voronoi diagram because of $|I| = 5$. Also, every straight line containing broken lines shown in Figure 4 passes through a point of $\mathbf{p}_i$'s, as in Figure 2.

The loci of $(F,G)(\partial V \cup L \cup \partial\Omega)$ and the trade-off curves $(F,G)(E^*)$ are depicted in Figure 5. The Pareto set consists of three polygonal paths. The optimal solutions of $F^2(\mathbf{x})$ and $G^2(\mathbf{x})$, denoted as $\mathbf{f}_2^*$ and $\mathbf{g}_2^*$, are located at one extreme of those paths. Contrary to Figure 3, the trade-off curve in Figure 5 is continuous between $(F,G)(\mathbf{f}_2^*)$ and $(F,G)(\mathbf{g}_2^*)$. A comparison of Figures 2 and 4 shows that the two Pareto sets are rather different, though the corresponding two two-objective problems are applicable to semi-obnoxious facility locations.

4. Convex Multicriteria Models

4.1. Problem formulation

In this section we consider that there are more than two convex quadratic ordered median criteria to be evaluated to determine the location of a facility on the feasible convex region Ω. Let Q be the index set of the quadratic ordered median criteria. So, $|Q|$ is the number of objectives. We will use superscript q to denote the q-th criterion for $q \in Q$. Here the following different quadratic convex ordered median problems are given:

$$\min_{\mathbf{x}\in\Omega} F^q(\mathbf{x}) \equiv \sum_{i\in I} \alpha_i^q \|\mathbf{x} - \mathbf{p}_{(i)}\|^2, \qquad q \in Q, \tag{18}$$

where $\alpha_1^q, \alpha_2^q, \cdots, \alpha_{|I|}^q$ are the weights for the q-th criterion. We define $A^q \equiv \sum_{i\in I} \alpha_i^q$. The convexity assumption of $F^q(\mathbf{x})$ then implies that $A^q \geq 0$ for any $q \in Q$.

By combining these $|Q|$ single-objective problems in (18), we have the following *quadratic distance convex multi-criteria ordered median problem*:

$$\min_{\mathbf{x}\in\Omega} \left\{F^1(\mathbf{x}), F^2(\mathbf{x}), \cdots, F^{|Q|}(\mathbf{x})\right\}. \tag{19}$$

As before, we would like to construct the set of Pareto solutions E^* for (19), but this goal does not seem to be easily reachable directly in general. Instead, we will rather show how to construct the set of weak-Pareto solutions, i.e. the set of points $\mathbf{x} \in \Omega$ such that for any $\mathbf{y} \in \Omega$ we have $F^q(\mathbf{y}) \geq F^q(\mathbf{x})$ for some $q \in Q$. Under the mild condition that there cannot be equivalent solutions (i.e. when $F^q(\mathbf{y}) = F^q(\mathbf{x})$ for all $q \in Q$ implies $\mathbf{x} = \mathbf{y}$) these two sets coincide. In what follows we will assume that this holds. It is easy to see that this will be the case in particular when all the objectives $F^q(\mathbf{x})$ are strictly convex (i.e. $A_q > 0$), or when the points $\mathbf{p}_i$ are in general position, in the following sense (extending the assumptions of the previous section):

(b-1) contour lines of any two objectives intersect in isolated points only;

(b-2) all F^q have unique minimum solutions in Ω, denoted by $\mathbf{f}_q^*$.

Therefore the (weak) Pareto set for the problem (19) is still denoted as E^*. The Pareto set for the two-objective problem associated with $F^q(\mathbf{x})$ and $F^r(\mathbf{x})$ is likewise denoted as E_{qr}^*, while for the three-objective problem associated with $F^q(\mathbf{x})$, $F^r(\mathbf{x})$ and $F^s(\mathbf{x})$ it is denoted as E_{qrs}^*.

4.2. Properties

Consider the following unconstrained convex vector minimization problem:

$$\min_{\mathbf{x}\in\mathbb{R}^2} \left\{F^1(\mathbf{x}), F^2(\mathbf{x}), \cdots, F^{|Q|}(\mathbf{x})\right\}.$$

The following facts about the set of weak-Pareto solutions $WE(F^1, F^2, \cdots, F^{|Q|})$ for this unconstrained problem with inf-compact objectives (i.e. having compact lower level sets) defined on the plane $\mathbb{R}^2$ are known from literature:

(r-1) for two objectives: $WE(F^q, F^r)$ is a connected set connecting the minimal solutions $\mathbf{f}_q^*$ and $\mathbf{f}_r^*$ of each single objective problem. Under the assumptions made above it will be more precisely a continuous curve connecting these two points (see Hansen et al.[13]).

(r-2) for three objectives: $WE(F^q, F^r, F^s)$ is the part of the plane enclosed by the weak-Pareto solution sets of each two-objective sub-problem, $WE(F^q, F^r)$, $WE(F^r, F^s)$ and $WE(F^s, F^q)$, see Rodríguez-Chía and Puerto[33].

(r-3) for more than three objectives: we have (see Plastria and Carrizosa[28], Rodríguez-Chía and Puerto[33])

$$WE(F^1, F^2, \cdots, F^{|Q|}) = \bigcup_{Q'\subset Q, |Q'|=3} WE(F^q, q \in Q').$$

However, the same results hold also for such multiple objective problems constrained to some convex compact subset $S \subset \mathbb{R}^2$, as readily follows from the following technical lemma. The proof makes use of several notions and results of convex analysis, for which we refer in general to the book of Hiriart-Urruty and Lemaréchal [14]

Lemma 4.1 *Let S be a compact and convex subset of $\mathbb{R}^d$. Consider the constrained multi-objective problem (P):*

$$\min\{F^1, F^2, \cdots, F^{|Q|} | \mathbf{x} \in S\},$$

where all $F^q(\mathbf{x})$ are convex inf-compact functions defined on $\mathbb{R}^d$. Then one can find convex inf-compact functions $G^q(\mathbf{x})$ on $\mathbb{R}^d$, such that the (weak-)Pareto set for the unconstrained multi-objective problem (P'):

$$\min\{G^1, G^2, \cdots, G^{|Q|} | \mathbf{x} \in \mathbb{R}^d\}$$

equals the (weak-)Pareto set of (P).

Proof For every $q \in Q$ we will construct a convex inf-compact function $G^q(\mathbf{x})$ defined on $\mathbb{R}^d$, such that $G^q(\mathbf{s}) = F^q(\mathbf{s})$ for all $\mathbf{s} \in S$, and any point $\mathbf{x} \notin S$ is strictly dominated by some point $\mathbf{x}' \in S$, i.e. $G^q(\mathbf{x}) > G^q(\mathbf{x}') = F^q(\mathbf{x}')$. This will clearly prove the claimed result.

We may choose a compact $C \subset \mathbb{R}^d$ containing S in its interior. Since C is compact, each $F^q(\mathbf{x})$ is Lipschitz on C; call $L > 0$ a common strict Lipschitz constant for all $F^q(\mathbf{x})$ on C, i.e. for all $\mathbf{x} \neq \mathbf{y} \in C$ we have $F^q(\mathbf{x}) - F^q(\mathbf{y}) < L\|\mathbf{x} - \mathbf{y}\|$.

For every $F^q(\mathbf{x})$, each $\mathbf{a} \in S$ and each subgradient $\mathbf{p} \in \partial F^q(\mathbf{a})$, we may now consider the following function:

$$f_q^{\mathbf{a},\mathbf{p}}(\mathbf{x}) \equiv \langle\ \mathbf{x} - \mathbf{a}\ ;\ \mathbf{p}\ \rangle + F^q(\mathbf{a}).$$

By definition of subgradients we know that $f_q^{\mathbf{a},\mathbf{p}}(\mathbf{x}) \leq F^q(\mathbf{x})$ for all $\mathbf{x} \in \mathbb{R}^d$. If we choose in particular $\mathbf{x} = \mathbf{a} + \epsilon\mathbf{p}$ for some $\epsilon > 0$ sufficiently small to have $\mathbf{x} \in C$, we obtain $\epsilon\|\mathbf{p}\|^2 = \langle\ \mathbf{x} - \mathbf{a}\ ;\ \mathbf{p}\ \rangle \leq F^q(\mathbf{x}) - F^q(\mathbf{a}) < L\|\mathbf{x} - \mathbf{a}\| = L\epsilon\|\mathbf{p}\|$ from which we immediately obtain $\|\mathbf{p}\| < L$. Let us then define

$$H^q(\mathbf{x}) \equiv \sup_{\mathbf{a}\in S;\mathbf{p}\in\partial F^q(\mathbf{a})} f_q^{\mathbf{a},\mathbf{p}}(\mathbf{x}),$$

which is well defined at all $\mathbf{x} \in \mathbb{R}^d$ because it is bounded above by $F^q(\mathbf{x})$. Note that we also have $H^q(\mathbf{s}) = F^q(\mathbf{s})$ for any $\mathbf{s} \in S$.

On the other hand we may define the function

$$J(\mathbf{x}) \equiv \sup_{\mathbf{b}\in bd\,S;\mathbf{q}\in N_S(\mathbf{b}):\|\mathbf{q}\|=L} \langle\ \mathbf{x} - \mathbf{b}\ ;\ \mathbf{q}\ \rangle,$$

which considers every boundary point $\mathbf{b} \in bd\,S$ combined with every vector $\mathbf{q}$ in the normal cone $N_S(\mathbf{b})$ of the convex set S at $\mathbf{b}$ with $\|\mathbf{q}\| = L$ (note that such $\mathbf{q}$ always exist). This supremum exists for any fixed $\mathbf{x} \in \mathbb{R}^d$ since it may be bounded above as follows: choose any fixed $\mathbf{s} \in S$ and let $R = \max_{\mathbf{b}\in bd\,S} \|\mathbf{s} - \mathbf{b}\|$ (which exists by compactness of $bd\,S$), then we have $\langle\ \mathbf{x} - \mathbf{b}\ ;\ \mathbf{q}\ \rangle \leq \|\mathbf{x} - \mathbf{b}\|\|\mathbf{q}\| \leq L(\|\mathbf{x} - \mathbf{s}\| + \|\mathbf{s} - \mathbf{b}\|) \leq L\|\mathbf{x} - \mathbf{s}\| + LR$. Note also that by definition of normal cone, for any $\mathbf{b} \in bd\,S$ and $\mathbf{q} \in N_S(\mathbf{b})$ we have that $\langle\ \mathbf{s} - \mathbf{b}\ ;\ \mathbf{q}\ \rangle \leq 0$ for all $\mathbf{s} \in S$, and therefore $J(\mathbf{s}) \leq 0$ for all $\mathbf{s} \in S$.

We now finally define for every $\mathbf{q} \in Q$ and $\mathbf{x} \in \mathbb{R}^d$

$$G^q(\mathbf{x}) = H^q(\mathbf{x}) + \max(0, J(\mathbf{x}))$$

and proceed by proving all the claimed properties of these functions.

First, as a pointwise supremum of affine functions, each $H^q(\mathbf{x})$ is convex on $\mathbb{R}^d$. For the same reason $J(\mathbf{x})$ is convex on $\mathbb{R}^d$, and therefore also $\max(0, J(\mathbf{x}))$. So $G^q(\mathbf{x})$ is a sum of convex functions, and therefore convex.

Second, let us show that $G^q(\mathbf{x})$ is inf-compact, for which it will be sufficient to prove that any lower level set $\{\mathbf{x} \in \mathbb{R}^d \mid G^q(\mathbf{x}) \leq K\}$ is bounded. To this end choose any fixed $\mathbf{a} \in S$. On the one hand, choosing any subgradient $\mathbf{p} \in \partial F^q(\mathbf{a})$, for which it was noted before that $\|\mathbf{p}\| < L$, we have $H^q(\mathbf{x}) \geq f_q^{\mathbf{a},\mathbf{p}}(\mathbf{x}) = \langle\ \mathbf{x} - \mathbf{a}\ ;\ \mathbf{p}\ \rangle + F^q(\mathbf{a}) \geq F^q(\mathbf{a}) - \|\mathbf{p}\|\|\mathbf{x} - \mathbf{a}\|$. On the other hand it is well-known that any $\mathbf{x} \notin S$ has a (unique) projection point $\mathbf{x}' \in S$, i.e. such that $\|\mathbf{x}' - \mathbf{x}\| \leq \|\mathbf{s} - \mathbf{x}\|$ for all $\mathbf{s} \in S$, and moreover $\mathbf{x}' \in bd\,S$ and $\mathbf{x}' - \mathbf{x} \in N_S(\mathbf{x}')$. Choosing $\mathbf{b} = \mathbf{x}'$ and $\mathbf{q} = L\frac{\mathbf{x}'-\mathbf{x}}{\|\mathbf{x}'-\mathbf{x}\|}$ we obtain $\langle\ \mathbf{x} - \mathbf{b}\ ;\ \mathbf{q}\ \rangle = L\|\mathbf{x}' - \mathbf{x}\|$, which proves that $J(\mathbf{x}) \geq L\|\mathbf{x}' - \mathbf{x}\| \geq L(\|\mathbf{x} - \mathbf{a}\| - \|\mathbf{x}' - \mathbf{a}\|)$. Summing we obtain $G^q(\mathbf{x}) \geq F^q(\mathbf{a}) - L\|\mathbf{x}' - \mathbf{a}\| + (L - \|\mathbf{p}\|)\|\mathbf{x} - \mathbf{a}\|$. Therefore, as soon as $G^q(\mathbf{x}) \leq K$ we have $\|\mathbf{x} - \mathbf{a}\| \leq \frac{K+LR-F^q(\mathbf{a})}{L-\|\mathbf{p}\|}$, which proves inf-compactness.

Third, for any $\mathbf{s} \in S$ we have already noted that $H^q(\mathbf{s}) = F^q(\mathbf{s})$ and $J(\mathbf{s}) \leq 0$, from which one immediately obtains $G^q(\mathbf{s}) = F^q(\mathbf{s})$.

Finally, let us show that any $\mathbf{x} \notin S$ is strictly dominated by its projection $\mathbf{x}'$ on S. Choosing $\mathbf{p} \in \partial F^q(\mathbf{x}')$, we have for every $q \in Q$, by definition of $H^q(\mathbf{x})$, that $H^q(\mathbf{x}) \geq f_q^{\mathbf{x}',\mathbf{p}}(\mathbf{x}) = \langle\, \mathbf{x}-\mathbf{x}' \,;\, \mathbf{p} \,\rangle + F^q(\mathbf{x}') \geq F^q(\mathbf{x}') - \|\mathbf{p}\|\|\mathbf{x}'-\mathbf{x}\|$. We saw above that $J(\mathbf{x}) \geq L\|\mathbf{x}'-\mathbf{x}\|$ and that $\|\mathbf{p}\| < L$, so we have

$$G^q(\mathbf{x}) \geq H^q(\mathbf{x}) + J(\mathbf{x}) \geq F^q(\mathbf{x}') + (L - \|\mathbf{p}\|)\|\mathbf{x}' - \mathbf{x}\| > F^q(\mathbf{x}') = G^q(\mathbf{x}'),$$

which terminates the proof. ∎

For convex two-objective problems defined by $q, r \in Q$, the results of Section 3, writing now L^{qr} for the line set L defined there, show that the (weak) Pareto set E^*_{qr} consists of edges of the graph $\partial V \cup L^{qr} \cup \partial\Omega$. The additional information in the result (r-1), that for convex objectives E^*_{qr} forms a continuous curve joining $\mathbf{f}^*_q$ with $\mathbf{f}^*_r$, allows for the following direct determination of the line segments forming this curve, by generalization of the 'steepest descent path' idea pointed out in Ohsawa et al.[23].

Starting from $\mathbf{f}^*_q$, and later on more generally from some reached vertex $\mathbf{a}$ of the graph $\partial V \cup L^{qr} \cup \partial\Omega$, we have to choose which edge to follow in order to finally reach $\mathbf{f}^*_r$, and in this process the value of $F^r(\mathbf{x})$ must steadily decrease, while that of $F^q(\mathbf{x})$ must increase. Each edge incident with the vertex $\mathbf{a}$ will correspond to some curve in the $(F^q(\mathbf{x}), F^r(\mathbf{x}))$-diagram starting from $(F^q(\mathbf{a}), F^r(\mathbf{a}))$ and it is the non-dominated one we have to choose. Comparing with Figures 3 and 5 (where we measure $F^q(\mathbf{x})$ on the horizontal axis, and $F^r(\mathbf{x})$ on the vertical one) we see that this latter is the edge yielding the steepest downward slope in the $(F^q(\mathbf{x}), F^r(\mathbf{x}))$-diagram. Every edge incident with the vertex $\mathbf{a}$ is a line segment parallel to some direction $\mathbf{e} \neq \mathbf{0}$, and the slope of its (F^q, F^r)-image at $(F^q(\mathbf{a}), F^r(\mathbf{a}))$ equals the change of $F^r(\mathbf{x})$ relative to that of $F^q(\mathbf{x})$ when moving from $\mathbf{a}$ in the direction $\mathbf{e}$, which is given by the expression

$$\frac{DF^r(\mathbf{a})(\mathbf{e})}{DF^q(\mathbf{a})(\mathbf{e})}, \tag{20}$$

where $DF^q(\mathbf{a})(\mathbf{e})$ denotes the directional derivative of $F^q(\mathbf{x})$ at the point $\mathbf{a}$ in the direction $\mathbf{e}$. Therefore at the vertex $\mathbf{a}$ we must always choose the edge of direction $\mathbf{e}$ that minimizes (20) among the $\mathbf{e}$ satisfying $DF^r(\mathbf{a})(\mathbf{e}) < 0$ and $DF^q(\mathbf{a})(\mathbf{e}) > 0$. In the exceptional case where the minimum is reached by several edges at $\mathbf{a}$, one can find the steepest direction by using the directional derivative of $F^q(\mathbf{x})$ of the second order at the point $\mathbf{a}$ because $F^q(\mathbf{x})$ is quadratic. In what follows we will call the so constructed path the *steepest descent path from* $\mathbf{f}^*_q$ *to* $\mathbf{f}^*_r$.

Note finally that the directional derivatives are easy to calculate: each point $\mathbf{a}$ and edge, given by direction $\mathbf{e}$, to consider lies in (or on the boundary of) some region $V_{i_1,i_2,\cdots,i_{|I|}}$ in which the expressions (4) for $A^q = 0$ and (6) for $A^q > 0$ are valid, yielding

$$DF^q(\mathbf{a})(\mathbf{e}) = \begin{cases} \langle\, \mathbf{e} \,;\, \hat{\mathbf{p}}^q_{i_1,i_2,\cdots,i_{|I|}} \,\rangle, & \text{if } A^q = 0, \\ 2A^q \langle\, \mathbf{e} \,;\, \overline{\mathbf{p}}^q_{i_1,i_2,\cdots,i_{|I|}} - \mathbf{a} \,\rangle, & \text{if } A^q > 0, \end{cases}$$

where the definitions (5) and (7) are adapted to $F^q(\mathbf{x})$ by using the α^q_k's.

Proposition 5 *The Pareto set E^* consists of some connected faces of the planar graph $\partial V \cup \left(\bigcup_{q\in Q}\bigcup_{r\in Q, q>r} L^{qr}\right) \cup \partial\Omega$.*

Proof Combining the results (r-2) and (r-3) implies that the Pareto set E^* has to be enclosed by Pareto sets of type E^*_{qr}. This together with Proposition 3 means that E^* has to consist of connected faces of the planar graph $\partial V \cup \left(\bigcup_{q\in Q}\bigcup_{r\in Q,q>r} L^{qr}\right) \cup \partial\Omega$. ∎

4.3. Solution procedure

Proposition 3 together with the proof of Proposition 5 yields the following algorithm to construct the geometrical description of the Pareto set E^* for the convex multi-criteria ordered median problem (19):

Algorithm 3

Step 1. Construct the planar graph $\partial V \cup \partial\Omega$, and identify the solutions $\mathbf{f}^*_q$ for all $q \in Q$.

Step 2. For each q and $r(\neq q)$, define the planar graph $\partial V \cup L^{qr} \cup \partial\Omega$, and then find E^*_{qr}, i.e., the steepest descent path from $\mathbf{f}^*_q$ to $\mathbf{f}^*_r$ on $\partial V \cup L^{qr} \cup \partial\Omega$.

Step 3. For each q, r and s, find E^*_{qrs}, i.e., the area enclosed by E^*_{qr}, E^*_{rs} and E^*_{sq}.

Step 4. E^* is the union of all the constructed E^*_{qrs}.

Proposition 6 *Under the assumption of strict convexity or general position, and for fixed $|Q|$, the Pareto set E^* can be found in $O(|I|^5 + |I||\partial\Omega|)$ time.*

Proof Step 1 can be done in $O(|I|^5 + |I||\partial\Omega|)$ by applying Algorithm 1 for the convex region Ω, as noted in Section 2. For each pair of q and r, the graph $\partial V \cup L^{qr} \cup \partial\Omega$ can be established in $O(|I|^5 + |I||\partial\Omega|)$ time because Ω is convex, as seen in Step 1 of Algorithm 3 in Ohsawa et al. [23]. Since there are $O(|I|^4 + |\partial\Omega|)$ edges in the graph, the steepest descent path can be found in $O(|I|^4 + |\partial\Omega|)$. Thus, Step 2 can be done in $O(|I|^5 + |I||\partial\Omega|)$. Since each steepest descent path has $O(|I|^4 + |\partial\Omega|)$ edges, the area enclosed by three paths can be determined in $O(|I|^4 + |\partial\Omega|)$. In conclusion, Algorithm 3 requires $O(|I|^5 + |I||\partial\Omega|)$. ∎

4.4. Computational experiments

For the sake of convenience, we use almost the same location data as Ohsawa et al.[23], shown in Figure 6, where five affected points are indicated as $\mathbf{p}_i$'s. The boundaries ∂V and $\partial\Omega$ are indicated by thin and chain lines, respectively. Here we examine the following four-objective problem

$$\min_{\mathbf{x}\in\Omega}\{F^1(\mathbf{x}), F^2(\mathbf{x}), F^3(\mathbf{x}), F^4(\mathbf{x})\}, \tag{21}$$

where

$$\begin{aligned}
F^1(\mathbf{x}) &\equiv \sum_{i\in I} \|\mathbf{x}-\mathbf{p}_i\|^2,\\
F^2(\mathbf{x}) &\equiv \sum_{i\in I}\sum_{j\in I} \left|\|\mathbf{x}-\mathbf{p}_i\|^2 - \|\mathbf{x}-\mathbf{p}_j\|^2\right|,\\
F^3(\mathbf{x}) &\equiv \max_{i\in I} \|\mathbf{x}-\mathbf{p}_i\|^2,\\
F^4(\mathbf{x}) &\equiv \max_{\bar{I}\subseteq I,|\bar{I}|=3} \left(\sum_{i\in\bar{I}} \|\mathbf{x}-\mathbf{p}_i\|^2\right).
\end{aligned}$$

The first and second criteria correspond respectively to Weber and minimization of mean difference problems. Hence they can be regarded as pull and equity criteria, respectively. The third is a simple center criterion, so it can be considered either as a pull or an equity criterion. And the fourth criterion is a k-centrum problem with $k = 3$. As indicated in Table 1, these four criteria are all convex.

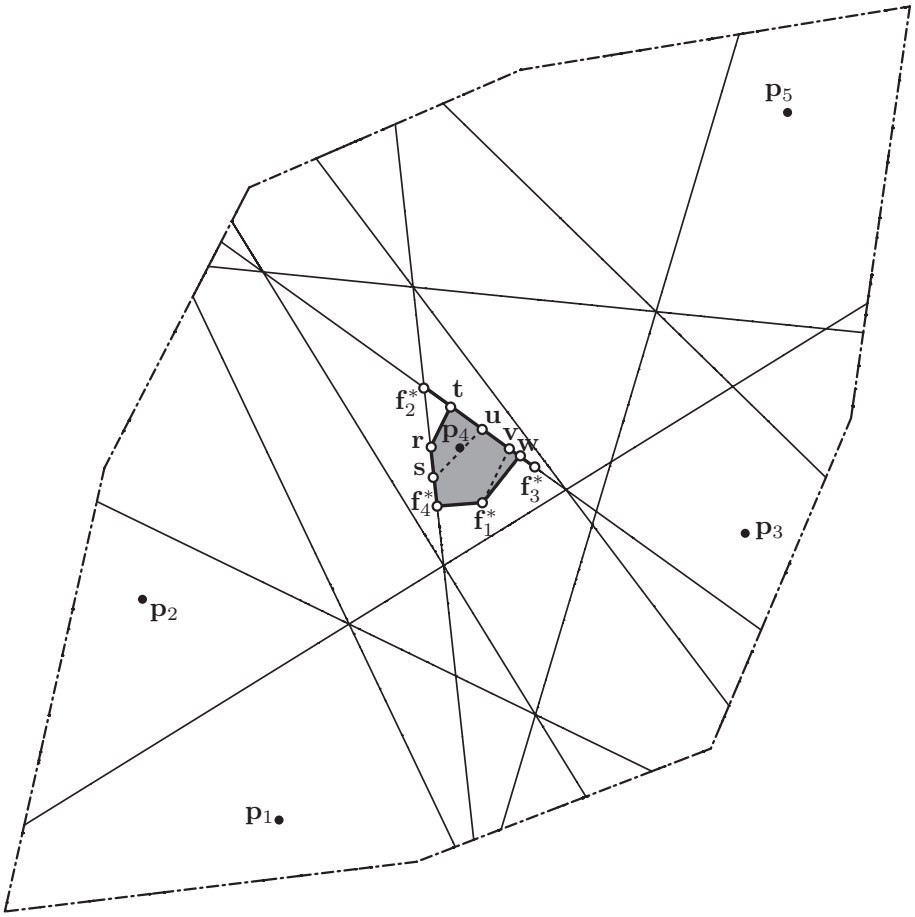

Figure 6: Pareto set for four-objective problem

In order to solve the four-objective problem (21) according to Algorithm 3, the following six two-objective sub-problems have to be separately solved:

$$\begin{aligned}
&\min_{\mathbf{x}\in\Omega}\{F^1(\mathbf{x}), F^2(\mathbf{x})\}, \qquad \min_{\mathbf{x}\in\Omega}\{F^1(\mathbf{x}), F^3(\mathbf{x})\},\\
&\min_{\mathbf{x}\in\Omega}\{F^1(\mathbf{x}), F^4(\mathbf{x})\}, \qquad \min_{\mathbf{x}\in\Omega}\{F^2(\mathbf{x}), F^3(\mathbf{x})\},\\
&\min_{\mathbf{x}\in\Omega}\{F^2(\mathbf{x}), F^4(\mathbf{x})\}, \qquad \min_{\mathbf{x}\in\Omega}\{F^3(\mathbf{x}), F^4(\mathbf{x})\}.
\end{aligned}$$

It should be noted that the first two problems were solved in Ohsawa et al.[23] and in Ohsawa[21], respectively.

As shown in Figure 6, the optimal solutions $\mathbf{f}_1^*$, $\mathbf{f}_2^*$, $\mathbf{f}_3^*$ and $\mathbf{f}_4^*$ are located within the Voronoi polygon $V_{5,1,2,3,4}$.

Figures 7, 8, 9 and 10 give different increased views of Figure 6. Here the thick lines indicate the two-objective Pareto sets connecting the corresponding one-objective optimal points.

The Pareto set E_{12}^* (E_{13}^* and E_{23}^*) is given by the polygonal path from $\mathbf{f}_1^*$ to $\mathbf{f}_2^*$ through the point $\mathbf{v}$ (the polygonal path from $\mathbf{f}_1^*$ to $\mathbf{f}_3^*$ through the point $\mathbf{w}$, and the line between $\mathbf{f}_2^*$ and $\mathbf{f}_3^*$). The Pareto set E_{14}^* (E_{24}^* and E_{34}^*) is given by the edge between $\mathbf{f}_1^*$ and $\mathbf{f}_4^*$ (the polygonal path from $\mathbf{f}_2^*$ to $\mathbf{f}_4^*$ through the points $\mathbf{t}$ and $\mathbf{r}$, the polygonal path from $\mathbf{f}_3^*$ to $\mathbf{f}_4^*$ through the points $\mathbf{u}$ and $\mathbf{s}$). Note that the segment $\overline{\mathbf{f}_1^*\mathbf{v}}$ ($\overline{\mathbf{f}_1^*\mathbf{w}}$, $\overline{\mathbf{rt}}$, $\overline{\mathbf{st}}$) is a subset of L^{12}(L^{13}, L^{24}, L^{34}), and the segments $\overline{\mathbf{f}_1^*\mathbf{v}}$ and $\overline{\mathbf{rt}}$ are parallel to each other.

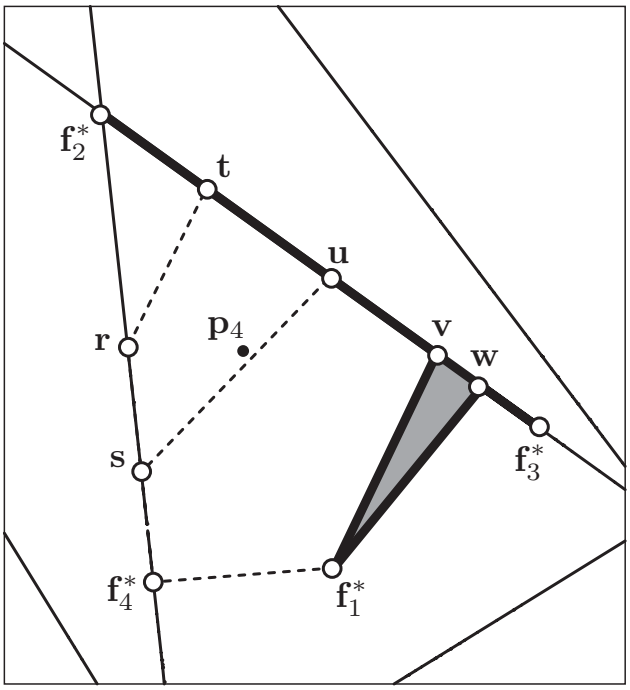

Figure 7: Pareto set E^*_{123}

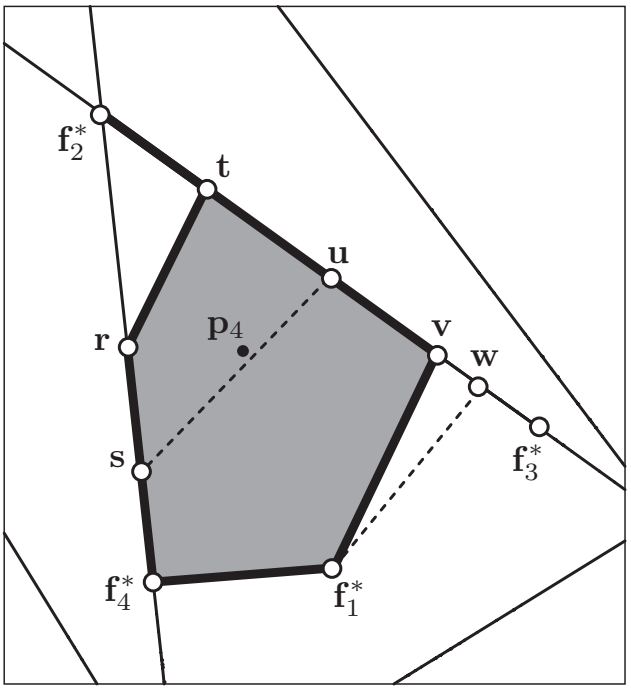

Figure 8: Pareto set E^*_{124}

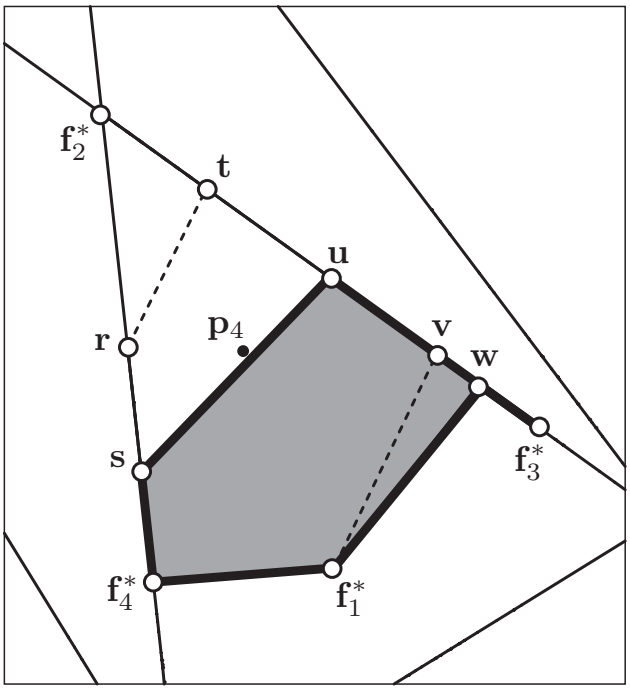

Figure 9: Pareto set E^*_{134}

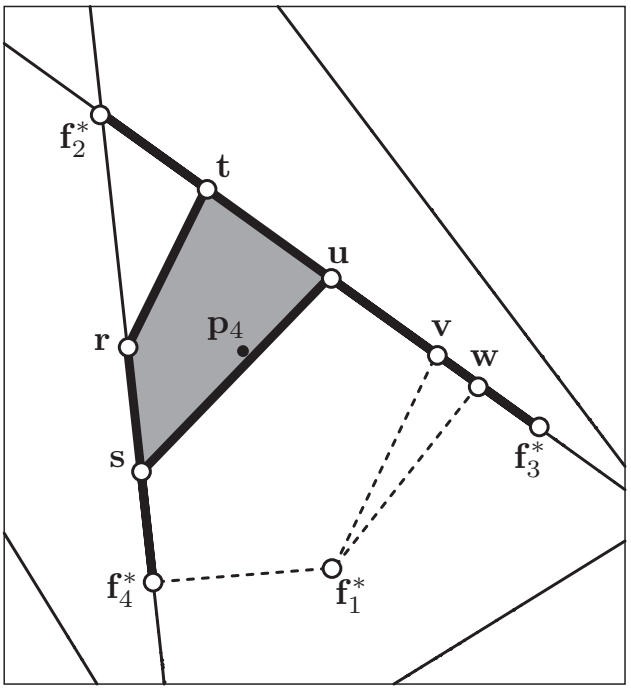

Figure 10: Pareto set E^*_{234}

Second, based on the two-objective Pareto sets E^*_{12}, E^*_{13}, E^*_{14}, E^*_{23}, E^*_{24} and E^*_{33}, we can find the Pareto sets associated with each of the following four sub-problems:

$$\min_{\mathbf{x}\in\Omega}\{F^1(\mathbf{x}), F^2(\mathbf{x}), F^3(\mathbf{x})\}, \qquad \min_{\mathbf{x}\in\Omega}\{F^1(\mathbf{x}), F^2(\mathbf{x}), F^4(\mathbf{x})\},$$
$$\min_{\mathbf{x}\in\Omega}\{F^1(\mathbf{x}), F^3(\mathbf{x}), F^4(\mathbf{x})\}. \qquad \min_{\mathbf{x}\in\Omega}\{F^2(\mathbf{x}), F^3(\mathbf{x}), F^4(\mathbf{x})\}.$$

The Pareto set associated with $\min_{\mathbf{x}\in\Omega}\{F^1(\mathbf{x}), F^2(\mathbf{x}), F^3(\mathbf{x})\}$, which is enclosed by E^*_{12}, E^*_{13} and E^*_{23}, is given by the segment $\overline{\mathbf{f}^*_2\mathbf{v}}$, the segment $\overline{\mathbf{f}^*_3\mathbf{w}}$, and the triangle with vertices $\mathbf{f}^*_1$, $\mathbf{v}$, $\mathbf{w}$, as shown in Figure 7. As exhibited in Figure 8, the Pareto set E^*_{124} consists of the pentagon with vertices $\mathbf{f}^*_1$, $\mathbf{f}^*_4$, $\mathbf{r}$, $\mathbf{t}$, $\mathbf{v}$, and the segment $\overline{\mathbf{f}^*_2\mathbf{t}}$. Figure 9 shows that the set E^*_{134} is given by the pentagon with vertices $\mathbf{f}^*_1$, $\mathbf{f}^*_4$, $\mathbf{s}$, $\mathbf{u}$, $\mathbf{w}$, and the segment $\overline{\mathbf{f}^*_3\mathbf{w}}$. The Pareto set E^*_{234} is given by the quadrilateral with vertices $\mathbf{s}$, $\mathbf{r}$, $\mathbf{t}$, $\mathbf{u}$ and the three segments $\overline{\mathbf{f}^*_2\mathbf{t}}$, $\overline{\mathbf{f}^*_3\mathbf{u}}$ and $\overline{\mathbf{f}^*_4\mathbf{s}}$, as shown in Figure 10.

The shaded area displayed in Figure 6 is the union of E^*_{123}, E^*_{124}, E^*_{134} and E^*_{234} and gives the Pareto set E^*. That is, the four-objective Pareto set is given by two segments $\overline{\mathbf{f}^*_2\mathbf{t}}$, $\overline{\mathbf{f}^*_3\mathbf{w}}$, and the pentagon with vertices $\mathbf{f}^*_1$, $\mathbf{f}^*_4$, $\mathbf{r}$, $\mathbf{t}$, $\mathbf{w}$.

Figure 6 clearly illustrates the well-known fact that the Pareto set expands as more criteria are used. For example, the optimal solution $\mathbf{f}^*_1$ is an element of the polygonal path E^*_{12}. This path is located within the Pareto area associated with E^*_{123}. This three-objective Pareto area is a subset of the four-objective Pareto area E^*.

5. Conclusions

Much attention has been given to ordered median location models, but relatively little to multi-objective formulations, in particular, non-convex cases. We present a polynomial-time algorithm to produce the Pareto-optimal solutions associated with many ordered median problems with the help of computational geometry such as Voronoi diagrams and arrangements of curves and lines. We devoted our discussion of ordered median problems to the squared Euclidean distances, but we expect that our results may quite easily be extended to other distances such as rectilinear distances, although more care will be needed in order to handle the difference between weak-Pareto and Pareto solutions.

Acknowledgment

This work was financed by the Research Grant of Japan Society for the Promotion of Science, Grant No. 18330057(2006). The authors have benefited from the comments of Masayasu Hachimori, Takafumi Kobayashi, Takeshi Koshizuka, Masashi Miyagawa and two reviewers of this journal.

References

[1] E. Carrizosa, E. Conde, F.R. Fernández and J. Puerto: An axiomatic approach to the cent-dian criterion. *Location Science*, **2** (1994), 165–171.

[2] E. Carrizosa and F. Plastria: Location of semi-obnoxious facilities. *Studies in Locational Analysis*, **12** (1999), 1–27.

[3] J.P. Crouzeix and R. Kebbour: On the convexity of some simple functions of ordered samples. *JORBEL: Belgian Journal of Operations Research, Statistics and Computer Sciences*, **36** (1996), 11–25.

[4] I. Das and J. E. Dennis: A closer look at drawbacks of minimizing weighted sums of objectives for Pareto set generation in multicriteria optimization problems. *Structural Optimization*, **14** (1997), 63–39.

[5] Z. Drezner, J.-F. Thisse and G.O. Wesolowsky: The minimax-min location problem. *Journal of Regional Science*, **26** (1986), 87–101.

[6] Z. Drezner and G.O. Wesolowsky: The Weber problem on the plane with some negative weights. *INFOR*, **29** (1991), 87–99.

[7] M. Ehrgott, H.W. Hamacher and S. Nickel: Geometric methods to solve max-ordering location problems. *Discrete Applied Mathematics*, **93** (1999), 3–20.

[8] H.A. Eiselt and G. Laporte: Objectives in location problems. In Z. Drezner (ed.): *Facility Location: A Survey of Applications and Methods* (Springer, Berlin, 1995), 151–180.

[9] F.R. Fernández, S. Nickel, J. Puerto and A.M. Rodriguez-Chia: Robustness in the Pareto-solutions for the multi-criteria minisum location problem. *Journal of Multi-Criteria Decision Analysis*, **10** (2001), 191–203.

[10] R.K. Francis and J.A. White: *Facility Layout and Location: An Analytical Approach* (Prentice-Hall, Englewood Cliffs, 1974).

[11] J. Halpern: The location of a center-median convex combination on an undirected tree. *Journal of Regional Science*, **16** (1976), 237–245.

[12] H.W. Hamacher and S. Nickel: Multicriteria planar location problems. *European Journal of Operational Research*, **94** (1996), 66–86.

[13] P. Hansen, D. Peeters and J.-F. Thisse: Constrained location and the Weber-Rawls problem. *Annals of Operations Research*, **11** (1981), 147–166.

[14] J.-B. Hiriart-Urruty and C. Lemaréchal: *Fundamentals of Convex Analysis* (Springer, Berlin, 2001).

[15] J. Kalcsics, S. Nickel, J. Puerto and A. Tamir: Algorithmic results for ordered median problems. *Operations Research Letters*, **30** (2002), 149–158.

[16] J. Muñoz-Pérez and J.J. Saameño-Rodríguez: Location of an undesirable facility in a polygonal region with forbidden zones. *European Journal of Operational Research*, **114** (1999), 372–379.

[17] S. Nickel and J. Puerto: A unified approach to network location problems. *Networks*, **34** (1999), 283–290.

[18] S. Nickel and J. Puerto: *Location Theory –A Unified Approach–* (Springer, Berlin, 2005).

[19] S. Nickel, J. Puerto and A.M. Rodríguez-Chía: MCDM location problems. In J. Figueira, S. Greco and M. Ehrgott (eds.): *Multiple Criteria Decision Analysis*: (Springer, New York, 2005), 761–795.

[20] W. Ogryczak and A. Tamir: Minimizing the sum of the K largest functions in linear time. *Information Processing Letters*, **85** (2003), 117–122.

[21] Y. Ohsawa: A geometrical solutions for quadratic bicriteria location models. *European Journal of Operational Research*, **114** (1999), 380–388.

[22] Y. Ohsawa: Bicriteria Euclidean location associated with maximin and minimax criteria. *Naval Research Logistics*, **47** (2000), 581–592.

[23] Y. Ohsawa, N. Ozaki and F. Plastria: Equity-efficiency bicriteria location with squared Euclidean distances. *Operations Research*, to appear.

[24] Y. Ohsawa, F. Plastria and K. Tamura: Euclidean push-pull partial covering problems. *Computers and Operations Research*, **33** (2006), 3566–3582.

[25] Y. Ohsawa and K. Tamura: Efficient location for a semi-obnoxious facility: *Annals of Operations Research*, **123** (2003), 173–188.

[26] T. Ohyama: Some Voronoi diagrams that consider consumer behavior analysis. *Japan Journal of Industrial and Applied Mathematics*, **22** (2005), 279–290.

[27] A. Okabe, B. Boots, K. Sugihara and S.N. Chiu: *Spatial Tessellations* (Wiley, New York, 1999).

[28] F. Plastria and E. Carrizosa: Geometrical characterization of weakly efficient points. *Journal of Optimization Theory and Applications*, **90** (1996), 217–223.

[29] J. Puerto and F.R. Fernández: A convergent approximation scheme for efficient sets of the multi-criteria Weber location problem. *Top*, **6** (1998), 195–204.

[30] J. Puerto and F.R. Fernández: Multi-criteria minisum facility location problems. *Journal of Multi-Criteria Decision Analysis*, **8** (1999), 268–280.

[31] J. Puerto and F.R. Fernández: Geometrical properties of the symmetrical single facility location problem. *Journal of Nonlinear and Convex Analysis*, **1** (2000), 321–342.

[32] A.M. Rodríguez-Chía, S. Nickel, J. Puerto and F.R. Fernández: A flexible approach to location problems. *Mathematical Methods of Operations Research*, **51** (2000), 69–89.

[33] A.M. Rodríguez-Chía and J. Puerto: Geometrical description of the weakly efficient solution set for multicriteria location problems. *Annals of Operations Research*, **111** (2002), 181–196.

[34] P.J. Slater: Centers to centroids in graphs. *Journal of Graph Theory*, **2** (1978), 209–222.

[35] A. Tamir: The k-centrum multi-facility location problem. *Discrete Applied Mathematics*, **109** (2001), 293–307.

Yoshiaki Ohsawa
Institute of Policy and Planning Sciences
University of Tsukuba
1-1-1 Tennoudai, Tsukuba 305-8573, Japan
E-mail: osawa@sk.tsukuba.ac.jp